Activity-dependent secretion of progranulin from synapses

Eugenia Petoukhov[1,4], Sarah Fernando[2], Fergil Mills[1,4], Farhan Shivji[1], Diana Hunter[2], Charles Krieger[3,4], Michael A. Silverman[2,4] and Shernaz X. Bamji[1,4,*]

[1]Department of Cellular and Physiological Sciences and the Brain Research Centre, University of British Columbia, 2350 Health Sciences Mall, Vancouver, BC, V6T-1Z3, Canada
[2]Department of Biological Sciences, Simon Fraser University, 8888 University Drive, Burnaby BC, V5A 1S6, Canada
[3]Department of Biomedical Physiology and Kinesiology, Simon Fraser University, 8888 University Drive, Burnaby BC, V5A 1S6, Canada
[4]Brain Research Center, University of British Columbia, 2211 Wesbrook Mall, Vancouver, BC Canada, V6T 2B5, Canada
*Author for correspondence (shernaz.bamji@ubc.ca)

Accepted 27 August 2013
Journal of Cell Science 126, 5412–5421

doi: 10.1242/jcs.132076

Summary

The secreted growth factor progranulin (PGRN) has been shown to be important for regulating neuronal survival and outgrowth, as well as synapse formation and function. Mutations in the PGRN gene that result in PGRN haploinsufficiency have been identified as a major cause of frontotemporal dementia (FTD). Here we demonstrate that PGRN is colocalized with dense-core vesicle markers and is co-transported with brain-derived neurotrophic factor (BDNF) within axons and dendrites of cultured hippocampal neurons in both anterograde and retrograde directions. We also show that PGRN is secreted in an activity-dependent manner from synaptic and extrasynaptic sites, and that the temporal profiles of secretion are distinct in axons and dendrites. Neuronal activity is also shown to increase the recruitment of PGRN to synapses and to enhance the density of PGRN clusters along axons. Finally, treatment of neurons with recombinant PGRN is shown to increase synapse density, while decreasing the size of the presynaptic compartment and specifically the number of synaptic vesicles per synapse. Together, this indicates that activity-dependent secretion of PGRN can regulate synapse number and structure.

Key words: Progranulin, Synapses, Activity, Secretion, Hippocampal culture, Protein trafficking, Frontotemporal dementia

Introduction

Progranulin (PGRN) is a multi-functional, secreted growth factor expressed in a variety of tissues throughout the body (Bateman and Bennett, 2009). In the adult brain, PGRN is expressed in microglia, in pyramidal neurons of the cortex and hippocampus, as well as in cerebellar Purkinje cells and spinal motor neurons (Petkau et al., 2010). PGRN has been shown to play a role in promoting neuronal survival, enhancing neurite outgrowth and regulating inflammation in the central nervous system (CNS) (Guo et al., 2010; Ryan et al., 2009; Tang et al., 2011; Van Damme et al., 2008; Xu et al., 2011). Interest in the regulation and function of PGRN in the brain has significantly increased following the discovery that mutations in the progranulin (also known as granulin) gene (*GRN*) are the major cause of autosomal dominant frontotemporal dementia (FTD) with tau-negative inclusions (Baker et al., 2006; Bronner et al., 2007; Cruts et al., 2006; Gass et al., 2006; Mukherjee et al., 2006; Pickering-Brown et al., 2006; van der Zee et al., 2007).

Most of the pathogenic mutations result in null alleles, and it is believed that frontotemporal dementia results from PGRN haploinsufficiency (Baker et al., 2006; Cruts et al., 2006). However, a number of FTD-linked mutations that specifically lead to deficiencies in PGRN secretion have also been identified (Mukherjee et al., 2008; Shankaran et al., 2008; Wang et al., 2010). A further understanding of the regulation of PGRN secretion is therefore warranted.

Previous work from our lab has demonstrated that knocking down PGRN levels in rat primary hippocampal cultures reduces neuronal arborization and the density of synapses, but enhances the size of presynaptic compartments and the frequency of mini excitatory postsynaptic currents (mEPSCs) of the remaining synapses (Tapia et al., 2011). In addition, PGRN knockout mice display altered synaptic connectivity, impaired synaptic plasticity and abnormal neuronal morphology (Petkau et al., 2012). Taken together, these data suggest PGRN has neurotrophic properties and plays an important role in regulating neuronal morphology and connectivity. Despite the recent interest in how PGRN functions in the brain, the regulation of PGRN transport and secretion have not yet been characterized in neurons.

We demonstrate that PGRN is localized to a subset of synapses in both axons and dendrites and is transported bi-directionally with transport characteristics similar to those of dense-core vesicles. In addition, we demonstrate that PGRN is highly colocalized and co-transported with a well-characterized neurotrophin, brain-derived neurotrophic factor (BDNF), and is further recruited to synapses following neuronal activity. Similar to that previously shown for BDNF, PGRN is secreted from axons and dendrites in an activity-dependent manner with different temporal profiles of secretion. This secretion is dependent on the activation of voltage-gated calcium channels (VGCC) and can be blocked in Ca^{2+}-free media or in the presence of VGCC blockers. Treatment of cultured hippocampal

neurons with recombinant PGRN results in increased synapse density. These results suggest that PGRN secretion may play a key role in regulating activity-dependent changes in neuronal connectivity.

Results

Expression of endogenous and fluorescently tagged PGRN

Immunostaining of cultured hippocampal neurons at 14 days *in vitro* (DIV) demonstrated that endogenous PGRN is distributed in a punctate pattern in both dendrites and axons, identified as thick MAP2-positive and thin MAP2-negative processes, respectively (Fig. 1A). To determine whether the punctate distribution of PGRN represents PGRN at synapses, we co-immunostained for the excitatory pre-synaptic maker, VGlut-1, and the excitatory post-synaptic marker, PSD-95 (Fig. 1C). Synapses were defined as points of colocalization between VGlut-1 and PSD-95. We found that 16±1.1% of endogenous PGRN puncta were localized to synapses (n=35 neurons, three cultures), indicating that the majority of PGRN is localized at extrasynaptic sites.

To validate the use of PGRN tagged with either GFP or its pH-sensitive variant, super ecliptic pHluorin (SEP) for studying activity-induced PGRN secretion, we examined the distribution of PGRN–GFP. This distribution was similar to that of endogenous PGRN, with a punctate pattern of PGRN–GFP in dendrites and axons (Fig. 1B). Moreover, the distribution of PGRN–GFP at excitatory synapses was similar to that of endogenous PGRN with 11.2±1.4% of PGRN–GFP puncta localized to synapses (Fig. 1D; n=30 neurons, three cultures). Using immunocytochemistry, cells transfected with PGRN–GFP were shown to express 2.3±0.35-fold more PGRN than non-transfected cells (n=6 neurons, two cultures; supplementary material Fig. S1). Together, these data demonstrate that fluorescently tagged PGRN is a faithful marker for endogenous PGRN, similar to that shown for many neuronal proteins.

Colocalization and co-transport of PGRN and BDNF

Progranulin is a secreted protein exhibiting neurotrophic functions including regulation of neuronal survival and neurite outgrowth (Ryan et al., 2009; Tapia et al., 2011; Van Damme et al., 2008). We next determined the relationship between PGRN and brain-derived neurotrophic factor (BDNF), another secreted trophic factor expressed in both axons and dendrites (Adachi et al., 2005; Jakawich et al., 2010; Matsuda et al., 2009), but see also Dieni et al. (Dieni et al., 2012). Cells expressing PGRN–GFP and BDNF–RFP were imaged at 8–10 DIV (Fig. 2A). The density of PGRN puncta in dendrites and axons was 82.4±5.9 and 52.2±2.6 puncta per 100 µm, respectively, and the density of BDNF puncta in dendrites and axons was 82.5±5.2 and 53.7±1.9 puncta per 100 µm, respectively (n=10 neurons, three cultures). There was a high degree of colocalization between PGRN and BDNF, with 84±2.4% of PGRN–GFP colocalizing with BDNF–RFP in dendrites and 91.7±2.6% in axons (Fig. 2A,B). Moreover, 82.4±2.9% of BDNF–RFP colocalized with PGRN–GFP in dendrites and 88.2±3.0% of BDNF–RFP colocalized with PGRN–GFP in axons (n=10 neurons, three cultures; Fig. 2A,B).

To examine the transport characteristics of PGRN, neurons were transfected with PGRN-GFP and imaged live using wide-field fluorescence microscopy. PGRN–GFP puncta were transported both anterogradely and retrogradely as evidenced by kymographs with positive and negative slopes, respectively, indicating that PGRN–GFP is trafficked bidirectionally in neurons (Fig. 2C). Quantification of the kymographs indicates that PGRN–GFP has transport characteristics consistent with that of microtubule-based dense-core vesicle (DCV) transport (Table 1) (Barkus et al., 2008; Kwinter et al., 2009). To determine whether PGRN and BDNF are transported together, neurons were co-transfected with PGRN-GFP and BDNF-RFP at 9 DIV and imaged live between 18 and 24 hours after transfection. We observed a substantial overlap in the movement of the two constructs in the axons of hippocampal neurons in anterograde and retrograde directions. The degree of co-transport was quantified and found to be close to 80% in both anterograde and retrograde directions (Fig. 2B). These values are comparable to the degree of overlap reported for other colocalization studies for DCVs (de Jong et al., 2008). In support of the idea that PGRN is transported in DCVs, we observed substantial colocalization between PGRN–GFP and the dense-core vesicle cargo protein, chromogranin A (ChromA–RFP; supplementary material Fig. S2A), as well as colocalization between endogenous and GFP-tagged PGRN, and the dense-core vesicle cargo protein, secretogranin II (SGII; supplementary material Fig. S2B,C). Although this data strongly suggests that

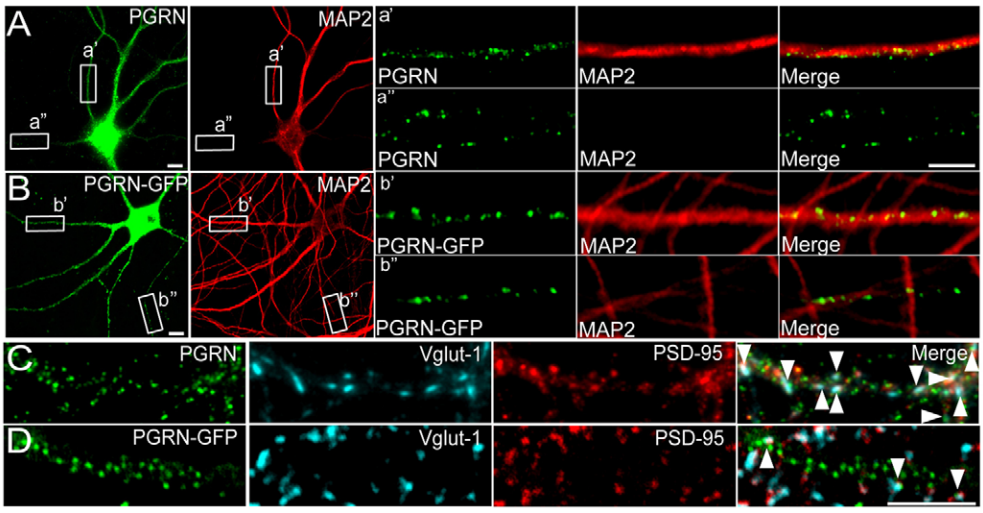

Fig. 1. PGRN is localized to a subset of synapses in axons and dendrites. Confocal images of 14 DIV hippocampal neurons. (A) Endogenous PGRN is expressed in a punctate distribution within MAP2-positive dendrites (a′) and MAP2-negative axons (a′′). (B) PGRN–GFP is similarly expressed in a punctate pattern within dendrites (b′) and axons (b′′). Neurons immunolabeled for PSD-95 and VGlut-1 demonstrate that a subset of endogenous PGRN (C) and PGRN–GFP (D) clusters are localized to excitatory synapses (arrowheads indicate points of triple colocalization). Scale bars: 5 µm.

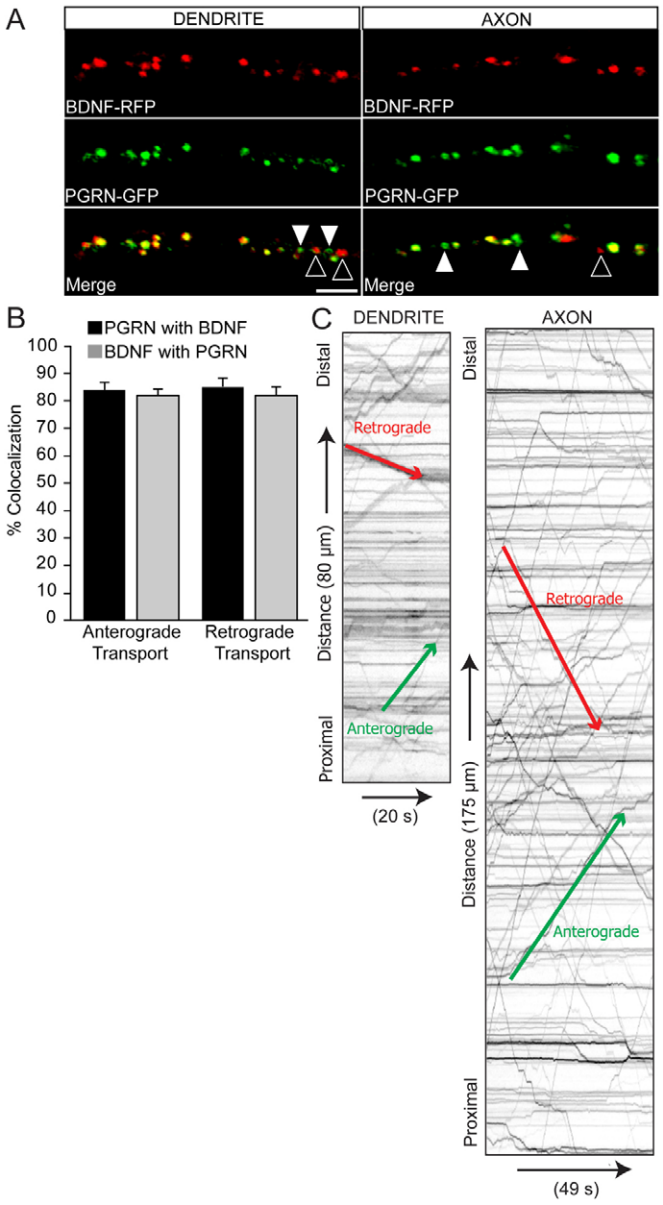

Fig. 2. PGRN–GFP and BDNF–RFP are co-transported anterogradely and retrogradely in axons and dendrites. (A) Confocal images of 14 DIV rat hippocampal neurons co-transfected with PGRN–GFP and BDNF–RFP. White arrowheads, PGRN–GFP puncta that do not colocalize with BDNF–RFP puncta. Black arrowheads, BDNF–RFP puncta that do not colocalize with PGRN–GFP puncta. Scale bar: 2 µm. (B) Approximately 80% of PGRN puncta are co-transported with BDNF both in the anterograde and retrograde direction. (C) Kymographs produced from a 'stream' acquisition of PGRN–GFP within the axon, depicting anterograde (green, positive slope) and retrograde (red, negative slope) movements (n=15 cells per condition, three experiments).

PGRN is transported in DCVs, immunoelectron microscopy is required to unequivocally confirm these findings.

Activity-induced translocation of PGRN

Previous work has demonstrated that activity enhances the recruitment of BDNF to synapses (Dean et al., 2012). To determine whether PGRN is also recruited to synapses following enhanced neuronal activity, we co-transfected neurons with PGRN-GFP and the pre-synaptic marker synaptophysin-RFP (synRFP) at 10 DIV and imaged neurons at 13 DIV. To enhance neuronal activity, cells were treated with 0.5 mM 4-aminopyridine (4-AP) plus 10 µm bicuculline and imaged 0, 5 and 10 minutes after treatment. 4-AP is a K^+ channel blocker, and enhances neuronal activity by increasing the amplitude and duration of action potentials (Alkadhi and Hogan, 1989). Bicuculline acts as a $GABA_A$ receptor antagonist, thus blocking the inhibitory input to the target neuron (Curtis et al., 1970). These compounds have been utilized together in a large number of studies to enhance neural activity (Hardingham et al., 2002; Hoey et al., 2009; Kuriu et al., 2006). We observed a significant (P<0.05) increase in the density of PGRN–GFP puncta 10 minutes after 4-AP and bicuculline treatment (labeled as '4-AP'), indicating that PGRN is recruited into axons following enhanced neural activity (Fig. 3A,C,D). In contrast, the density of synRFP remained unchanged providing a control for the specificity of activity-induced recruitment of PGRN into axons (Fig. 3A,C).

Activity also enhanced the recruitment of PGRN to synapses. Indeed, 26.3±3% of synRFP puncta that did not contain PGRN–GFP prior to stimulation, were associated with PGRN–GFP 10 minutes after stimulation (n=11 cells, three experiments). Moreover, we observed a significant (P<0.01) increase in the integrated density (product of the mean gray value and area) of PGRN–GFP puncta that were already at synapses, 5 and 10 minutes after stimulation (Fig. 3B–D). The increased integrated density of PGRN–GFP at synapses, and localization of PGRN–GFP to synRFP clusters not initially associated with PGRN, together demonstrate an activity-dependent recruitment of PGRN to synapses (Fig. 3C,D).

Activity enhances PGRN secretion

Previous work has demonstrated that activity enhances the secretion of BDNF from axons and dendrites (Dean et al., 2009; Lessmann and Brigadski, 2009; Matsuda et al., 2009). To determine whether PGRN is similarly secreted from cultured hippocampal neurons, we transfected neurons with a vector expressing PGRN fused to SEP, a pH-sensitive marker for vesicular exocytosis (Gandhi and Stevens, 2003; Miesenböck et al., 1998; Sankaranarayanan et al., 2000). The fluorescence of SEP is quenched at pH <6 and therefore not visible while inside the acidic lumen of a secretory vesicle, which has a pH of ~5.5 (Mellman et al., 1986; Njus et al., 1986). When the acidified vesicle fuses with the plasma membrane, the vesicle lumen undergoes a rapid increase in pH to ~7.4 resulting in the unquenching of SEP fluorescence (Miesenböck et al., 1998). PGRN–SEP puncta were sparsely distributed in both dendrites and axons (supplementary material Fig. S3A,B). To demonstrate that these few PGRN–SEP puncta represent unquenched PGRN–SEP at the cell surface, cultures were treated for 1 minute with an acidic solution containing 2-(*N*-morpholino)ethanesulfonic acid (MES), pH 5.2. Following MES treatment, we observed a rapid decrease in PGRN–SEP fluorescence in both dendrites and axons (supplementary material Fig. S3A,B). To demonstrate that PGRN–SEP fluorescence was quenched in the majority of vesicles, cells were treated with a solution of 50 mM NH_4Cl (pH 7.4), which has been demonstrated to rapidly diffuse across cell membranes and neutralize the acidic vesicular lumen (Miesenböck et al., 1998). Following a 1 minute application of

Table 1. Transport characteristics of PGRN-GFP in axons and dendrites of 14 DIV hippocampal neurons

	All events (n=67)	Anterograde events (n=43)	Retrograde events (n=24)
Axon			
Flux (per minute)	4.95±0.66	2.68±0.43	2.27±0.27
Velocity (μm/s)	1.73±0.06	1.70±0.07	1.73±0.07
Run length	6.19±0.32	6.61±0.51	5.73±0.24
Dendrite			
Flux (per minute)	2.46±0.60	1.61±0.53	0.86±0.19
Velocity (μm/s)	1.06±0.11	1.03±0.13	1.03±0.10
Run length	4.71±0.63	4.44±0.68	4.48±0.64

Values are from 11 kymographs and 11 cells (means ± s.e.m.).

NH_4Cl, we observed an increase in the number of fluorescent PGRN–SEP puncta in axons and dendrites at both synapses and extrasynaptic sites, suggesting that the majority of PGRN is localized intracellularly (supplementary material Fig. S3A,B).

To determine whether PGRN secretion is regulated by neuronal activity, the change in SEP fluorescence following enhanced activity was monitored using time-lapse confocal imaging. Specifically, cells were transfected with superecliptic pHluorin-tagged PGRN (PGRN-SEP) to visualize exocytotic events and either synRFP or PSD-95–RFP to demarcate synapses in axons and dendrites, respectively. Cells were imaged for 5 minutes in a low KCl solution to obtain baseline levels of PGRN secretion (see Materials and Methods) and then switched to a solution containing 70 mM KCl, or 0.5 mM 4-AP and 10 μM bicuculline and imaged every 12 seconds for 10 minutes. The average density of PGRN–SEP fluorescent puncta rapidly increased in axons following treatment with 4-AP and bicuculline, and was maintained throughout the imaging period

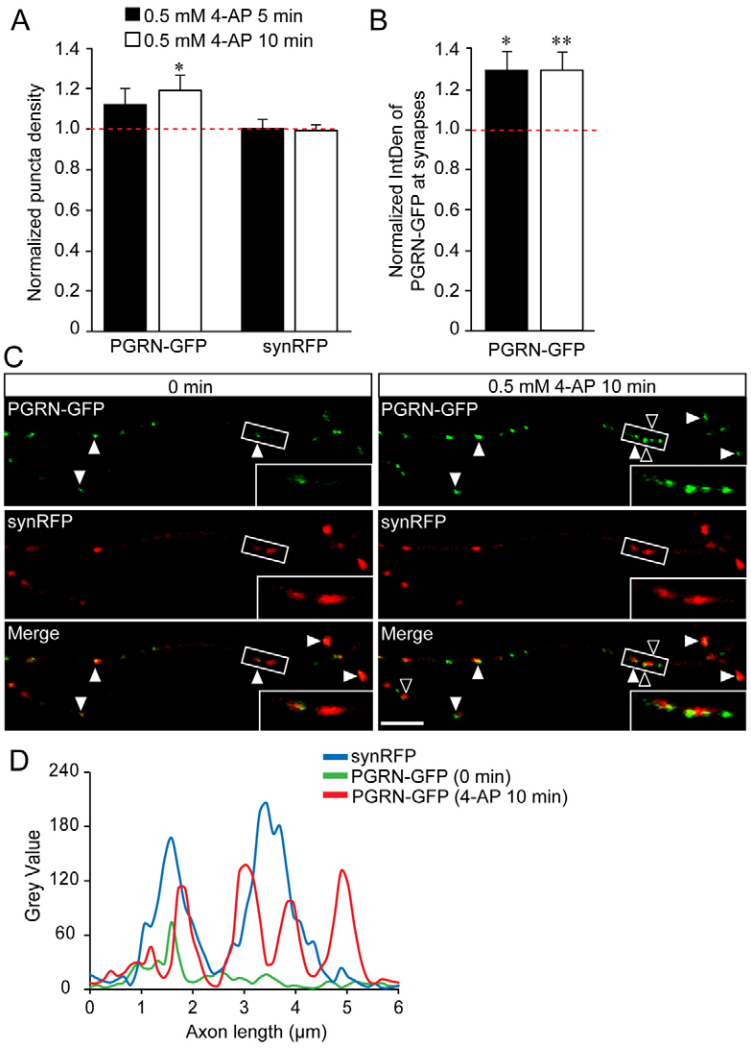

Fig. 3. Activity increases the density of PGRN–GFP puncta at axons and enhances the recruitment of PGRN–GFP to synapses. (A) The density of PGRN–GFP puncta in axons is increased at 10 minutes after treatment with 4-AP and bicuculline (labeled as '4-AP'; normalized to controls). Conversely, the density of synRFP puncta is unchanged (n=8–14 neurons per condition, three cultures). (B) The integrated density of PGRN–GFP puncta that are specifically colocalized with synRFP puncta is increased at 5 minutes and 10 minutes following 4-AP and bicuculline treatment (normalized to controls; n=8–14 neurons per condition, three cultures). *P<0.05, **P<0.01, Student's t-test. (C) Confocal images of 14 DIV hippocampal neurons co-transfected with PGRN-GFP and synRFP, before treatment and 10 minutes following treatment with 4-AP and bicuculline. White arrowheads indicate existing PGRN–GFP puncta colocalized with synRFP that increase in integrated density by 10 minutes after activity induction. Black arrowheads indicate PGRN–GFP puncta that are newly recruited to synRFP puncta. Scale bar: 5 μm. (D) Fluorescence distribution histogram depicting mean gray value of PGRN–GFP and synRFP puncta along a length of axon (from inset in C).

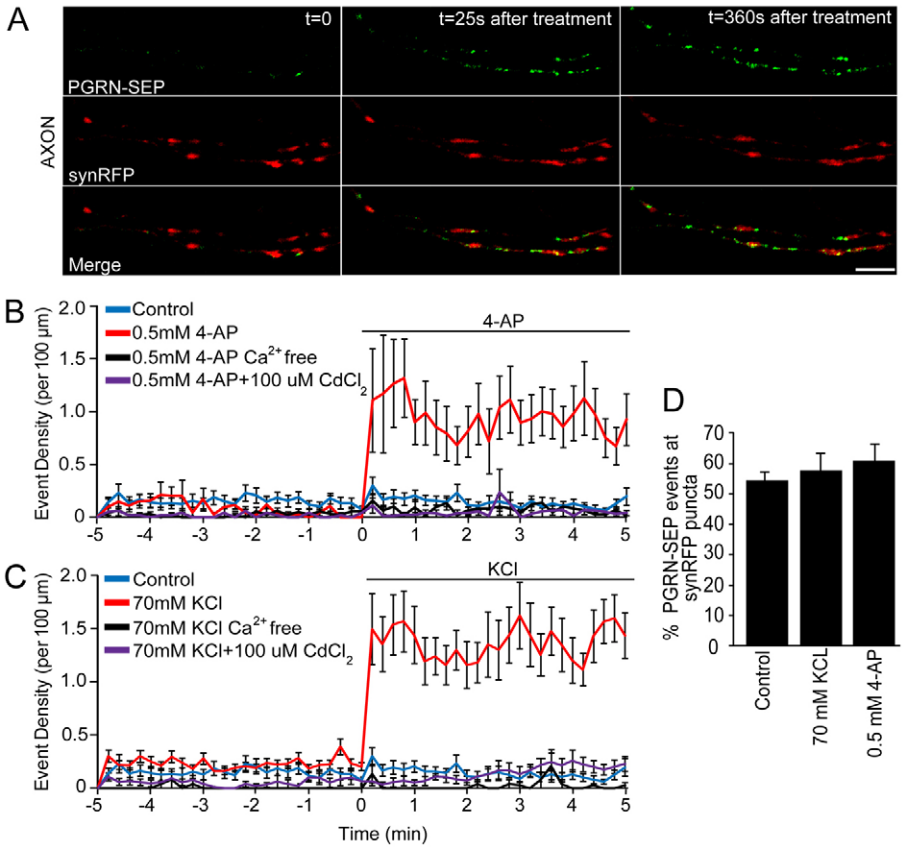

Fig. 4. Activity enhances the secretion of PGRN from axons. (A) Confocal images of 14 DIV hippocampal axons expressing PGRN–SEP and synRFP before and following stimulation with 4-AP and bicuculline. There is an increase in the average density of PGRN–SEP fluorescent events in axons following stimulation with 4-AP and bicuculline (B) or 70 mM KCl (C). This is abolished in Ca^{2+}-free medium or in the presence of $CdCl_2$ ($n=10$–23 neurons per condition, three cultures). $P<0.001$, two-way ANOVA with Bonferroni post-hoc test. (D) There is no significant difference in the proportion of PGRN–SEP fluorescent events at synRFP puncta after stimulation with KCl or 4-AP and bicuculline ($n=10$ neurons per condition, three cultures). $P>0.05$, Student's t-test. Scale bar: 5 µm.

(Fig. 4A,B). There was also a dramatic increase in the average density of PGRN–SEP fluorescent puncta in axons following stimulation with 70 mM KCl, which was similar in magnitude and time course of response to that observed following 4-AP and bicuculline stimulation (Fig. 4C).

To examine the role of Ca^{2+} in activity-mediated exocytosis of PGRN-containing vesicles, we stimulated the cells in Ca^{2+}-free medium and examined the average density of PGRN–SEP fluorescent puncta. Stimulating cells with 4-AP and bicuculline or 70 mM KCl in Ca^{2+}-free medium abolished activity-mediated increase in PGRN–SEP fluorescent events (Fig. 4B,C). In addition, blocking voltage-gated calcium channels (VGCCs) with $CdCl_2$ similarly abolished activity-mediated increase in the density of PGRN–SEP fluorescence events (Fig. 4B,C). Despite the minimal number of secretion events under basal conditions (0.155 ± 0.006 events per 100 µm in a 10 minute period, $n=33$ cells), this was further reduced in the absence of Ca^{2+} (0.099 ± 0.008 events per 100 µm in a 10 minute period; $n=22$ cells; $P<0.005$ Student's t-test). These data suggest that Ca^{2+} influx through the VGCC is necessary for activity-dependent fusion of PGRN–SEP-containing vesicles. To determine whether PGRN is preferentially secreted at synapses following activity, we analyzed the number of PGRN–SEP puncta that emerged at synRFP puncta. We observed a significant ($P<0.001$) increase in the number of PGRN–SEP events at synapses, however, the proportion of PGRN–SEP events at synapses was not significantly altered following activity induction (Fig. 4D).

We next examined whether activity induced a similar enhancement of PGRN–SEP events in dendrites. Similar to that observed in axons, treatment with 4-AP and bicuculline triggered a rapid increase in the density of PGRN–SEP fluorescent events within dendrites (Fig. 5A,B). However, unlike in the axons, the increase in the density of PGRN–SEP events was transient, and was not significantly different from prestimulation levels by 1.8 minutes after treatment with 4-AP and bicuculline. The differences in the temporal profiles of PGRN–SEP fluorescent events following activity in axons and dendrites may be due to different modes of secretion. Stimulation of cells in Ca^{2+}-free medium or in the presence of $CdCl_2$ abolished the activity-induced increase in PGRN–SEP events (Fig. 5A,B). These data suggest that Ca^{2+} influx through the VGCC is necessary for activity-dependent fusion of PGRN–SEP-containing vesicles in both axons and dendrites.

To determine whether PGRN is preferentially secreted at postsynaptic sites following activity, we analyzed the number of PGRN–SEP events at PSD-95–RFP puncta. Similar to that observed in axons, we observed no significant difference in the proportion of PGRN–SEP events at PSD-95 clusters (Fig. 5C), indicating that PGRN is not preferentially secreted from synapses following activity. Interestingly, PGRN secretion at extrasynaptic sites did not appear to mediate the recruitment of synaptic markers to sites of PGRN secretion. We therefore do not believe that PGRN secretion acts as a 'tag' for the formation of new synapses.

Recombinant PGRN treatment increases synapse density but decreases the size of presynaptic compartments

To examine the effects of secreted PGRN on synapse density and morphology, we treated hippocampal cultures with different concentrations of recombinant PGRN (rPGRN). Cells were treated with rPGRN at 0, 3, 7 and 10 DIV, transfected with

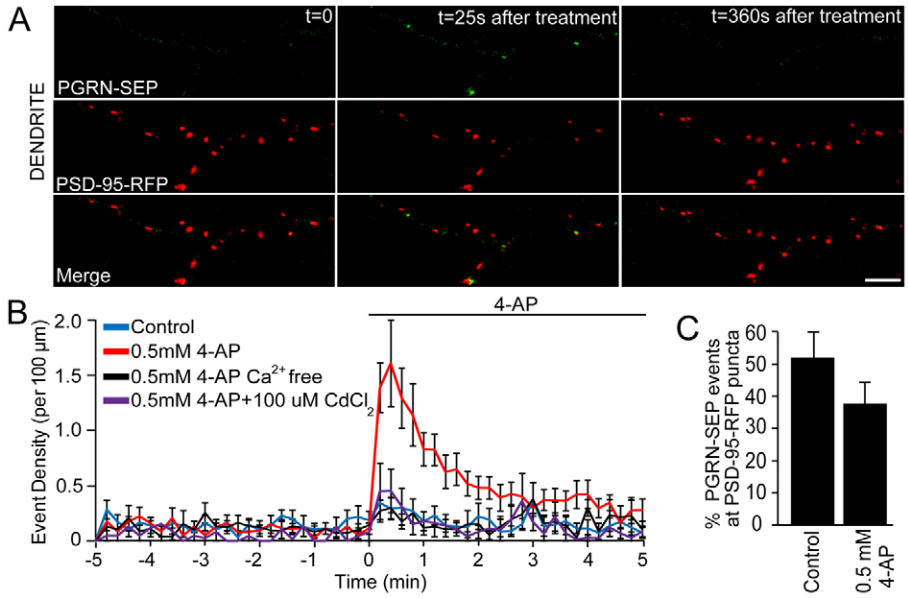

Fig. 5. Activity enhances the secretion of PGRN from dendrites. (A) Confocal images of 14 DIV hippocampal dendrites expressing PGRN–SEP and PSD-95–RFP before and following stimulation with 4-AP and bicuculline. (B) There is a transient increase in the average density of PGRN–SEP fluorescent events in dendrites following stimulation with 4-AP and bicuculline. This is abolished in Ca^{2+}-free medium or in the presence of $CdCl_2$ (n=9–28 neurons per condition, three cultures). $P<0.001$; two-way ANOVA with Bonferroni post-hoc test. (C) There is no significant difference in the proportion of PGRN–SEP fluorescent events at PSD-95–RFP puncta following stimulation with 4-AP and bicuculline (n=10 neurons per condition, three cultures). $P>0.05$, Student's t-test. Scale bar: 5 µm.

GFP at 10 DIV, fixed and immunolabeled for PSD-95 and VGlut-1 at 14 DIV (Fig. 6A–C). The density of synapses, defined by colocalized PSD-95 and VGlut-1 puncta within the GFP mask, was analyzed for each cell. We observed a small but significant increase in synapse density following treatment with 250 ng/ml PGRN (control: 10.9±0.50, rPGRN: 13.3±0.45 synapses/100 µm 0; $P<0.001$, Student's t-test; n=24 cells, three cultures; Fig. 6A,D). The integrated density of PSD-95 puncta was unaffected by rPGRN treatment (Fig. 6B,D); however, treatment with 250 ng/ml rPGRN resulted in a significant decrease in the integrated density of VGlut-1 puncta (control: 41.6±3.70, 250 ng rPGRN: 32.2±2.60; $P<0.05$, Student's t-test; n=24 cells, three cultures; Fig. 6C,D). This correlated with a significant decrease in the number of synaptic vesicles per synapse in PGRN-treated cells (control: 81.6±7.0 vesicles per synapse, 250 ng rPGRN: 64.5±4.0; $P<0.05$, Student's t-test; $n>50$ synapses; Fig. 6E,F). These results are consistent with our previous findings demonstrating a significant decrease in synapse density and increase in the size of Vglut- and synaptophysin-immunopositive puncta and the number of synaptic vesicles per synapse following PGRN knockdown (Tapia et al., 2011).

Discussion

Previous work has demonstrated an important role for PGRN in promoting neuronal survival and outgrowth, as well as in modulating neuronal connectivity (Gao et al., 2010; Guo et al., 2010; Petkau et al., 2012; Ryan et al., 2009; Tapia et al., 2011; Van Damme et al., 2008). PGRN is normally expressed in a large number of neuronal populations in the adult CNS (Petkau et al., 2010); however, acute and chronic insults to the CNS, including neurodegenerative disorders such as FTD, result in a dramatic upregulation of PGRN in microglia, suggesting that PGRN may play a key role in regulating the neuroinflammatory response (Mackenzie et al., 2006; Matzilevich et al., 2002).

Our findings demonstrate that PGRN is co-transported with BDNF in axons and dendrites with transport characteristics resembling those of DCVs. We show that activity induces the recruitment of PGRN into axons and specifically induces the recruitment of PGRN to presynaptic compartments. Activity also induces the secretion of PGRN from both axons and dendrites and at both synaptic and extrasynaptic sites. Despite the fact that axons and dendrites exhibit distinct temporal profiles of activity-induced PGRN secretion, secretion from both compartments requires activation of VGCCs and an increase in intracellular Ca^{2+}. This is consistent with that reported for regulated BDNF secretion (Balkowiec and Katz, 2002; Goodman et al., 1996; Hartmann et al., 2001; Santi et al., 2006). Finally, we have demonstrated that treatment of neurons with recombinant PGRN results in an increase in synapse density and a decrease in the size of presynaptic compartments, complementing our previous findings in PGRN knockdown cells (Tapia et al., 2011).

Neuropeptides are packaged in the Golgi apparatus and then trafficked to sites of release. We find that BDNF and PGRN are co-transported in both axons and dendrites, and appear to be similarly recruited to synapses following enhanced neuronal activity. Disruptions in BDNF transport have been reported in a number of disease states including Huntington's disease, focal ischemia, glaucoma, Alzheimer's disease and Rett syndrome (Gauthier et al., 2004; Kokaia et al., 1998; Pease et al., 2000; Poon et al., 2011; Roux et al., 2012). As PGRN and BDNF are transported together in vesicles, it is possible that they exert similar or complementary functions in maintaining neuronal survival and regulating synaptic function.

Previous work by Dean and colleagues showed that BDNF is recruited to synapses following increased neuronal activity (Dean et al., 2012), which is similar to our findings for PGRN. These observations suggest that in addition to increasing protein synthesis and trafficking of neurotrophins to distal sites, activity can capture vesicles at active synapses, where it may act to rapidly modulate synaptic strength. This phenomenon has also been observed at the *Drosophila* neuromuscular junction, where increased neuronal activity results in the recruitment of peptidergic vesicles to synaptic boutons (Shakiryanova et al., 2006). In addition, it has been previously demonstrated that stimulating hippocampal neurons with KCl results in increased dendritic localization of BDNF mRNA (Tongiorgi et al., 1997).

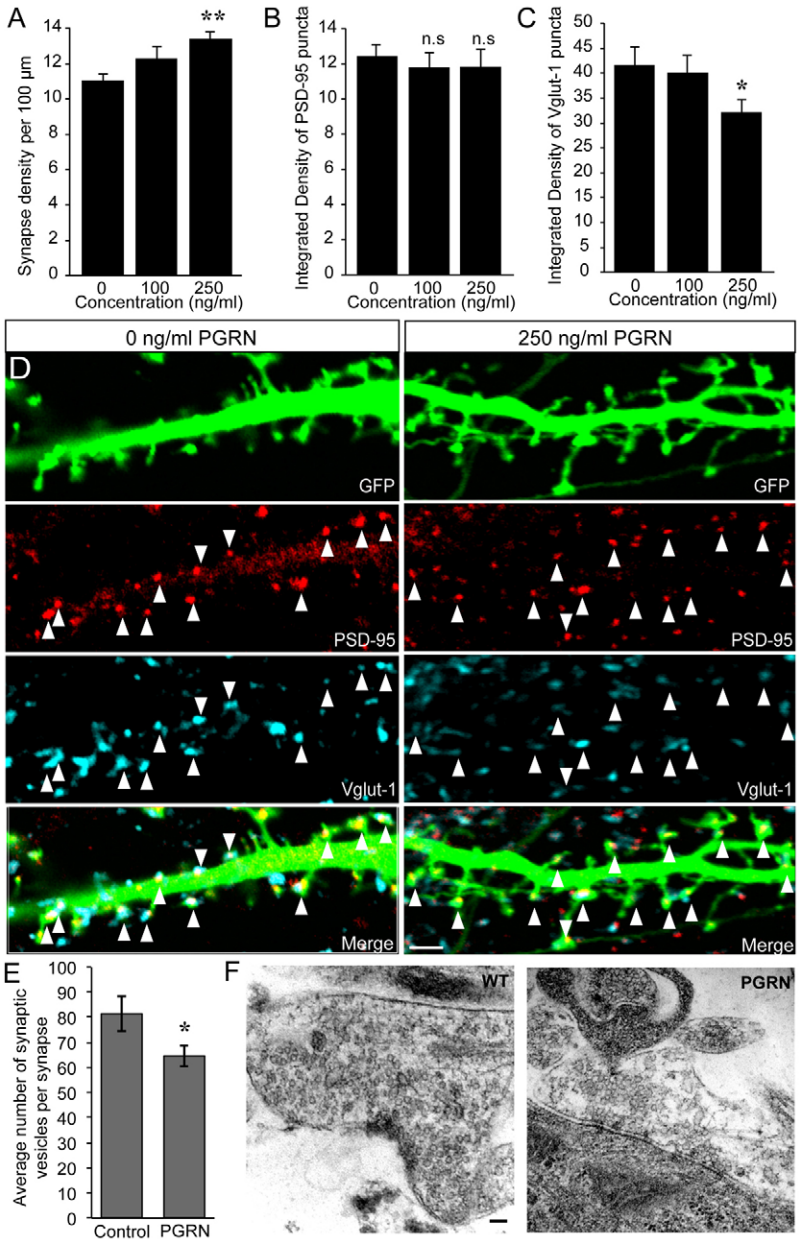

Fig. 6. Synapse density is increased, but integrated density of VGlut-1 puncta is decreased following treatment with recombinant PGRN. (A) The density of synapses, determined by the density of colocalized VGlut-1 and PSD-95 clusters along a GFP mask, is significantly increased following treatment with 250 ng/ml rPGRN. (B) The integrated density of PSD-95 puncta is unchanged following treatment with rPGRN. (C) The integrated density of VGlut-1 puncta is significantly decreased following treatment with 250 ng/ml rPGRN (n=24 cells per condition, three cultures).*P<0.05, **P<0.01; Student's t-test. (D) Confocal images of 14 DIV hippocampal neurons transfected with GFP and immunolabeled for PSD-95 and Vglut-1, treated with either 0 ng/ml rPGRN (left panel) or 250 ng/ml rPGRN (right panel). White arrowheads indicate points of colocalization between PSD-95 and Vglut-1 puncta within a single, GFP-transfected neuron. Scale bar: 2 µm. (E) The number of synaptic vesicles per synapse is decreased in cells treated with 250 ng/ml rPGRN (n=54–58 synapses per condition). *P<0.05, Student's t-test. (F) Electron microscopy images of synapses treated with either 0 ng/ml rPGRN (left panel) or 250 ng/ml PGRN (right panel). Scale bar: 100 nm.

Similar to what we have shown for PGRN, BDNF is secreted from axons and dendrites in an activity-dependent manner, and this is dependent on the activation of VGCC and an increase in intracellular Ca^{2+} concentration (Balkowiec and Katz, 2002; Goodman et al., 1996; Hartmann et al., 2001; Santi et al., 2006). We have demonstrated that PGRN is released with different temporal profiles of secretion from axons and dendrites. Although activity results in a rapid increase in PGRN–SEP fluorescent events in both axons and dendrites, in axons the number of PGRN–SEP events is maintained for the duration of 4AP and bicuculline treatment, whereas in dendrites the number of PGRN–SEP fluorescent events decreases sharply over time. Previous studies have also reported different modes of activity-mediated BDNF release in axons and dendrites. BDNF secretion events in dendrites have been shown to be larger and faster than in axons, indicating full fusion of BDNF-containing vesicles (Dean et al., 2009; Matsuda et al., 2009). In contrast, the characteristics of axonal BDNF release events following activity correspond to partial fusion of BDNF-containing vesicles, indicating the kiss-and-run mode of BDNF release (Dean et al., 2009; Matsuda et al., 2009). Indeed, the recycling of vesicles following multiple kiss-and-run events at the axon may explain the sustained levels of PGRN–SEP fluorescent events in the axon following stimulation. Conversely, complete fusion of PGRN–SEP-containing vesicles in the dendrites may account for the decay in the average density of PGRN–SEP fluorescent events after the initial activity-induced increase.

Axonal and dendritic PGRN vesicles may in fact belong to two distinct populations, which may also contribute to different activity-induced PGRN release profiles in the axonal and dendritic compartments. Accordingly, it has been previously shown that distinct subsets of BDNF-containing vesicles are differentially sorted to axons and dendrites (Dean et al., 2012).

It has been previously suggested that presynaptic and postsynaptic BDNF release may differentially affect synaptic function. Indeed, presynaptic BDNF secretion increases only presynaptic strength, whereas postsynaptic BDNF secretion increases both postsynaptic and presynaptic strength (Dean et al., 2009). It is possible that the different modes of activity-mediated secretion of PGRN from the axon and dendrites may also have distinct effects on synaptic function; however, this has yet to be tested.

In addition to distinct methods of BDNF sorting and release in axons and dendrites, there is evidence that BDNF can be secreted constitutively as well as its well-described regulated release (Lessmann and Brigadski, 2009; Lu et al., 2005). Indeed, a recent study has demonstrated that acute and gradual increases in BDNF concentration activate different intracellular cascades, leading to differences in spine morphology (Ji et al., 2010). These results suggest that it is not only the concentration of secreted BDNF that is important in the regulation of neuronal function and morphology, but also the manner in which it is secreted: constitutively or in response to neuronal activity. It is possible that constitutive and regulated secretion of PGRN also differentially regulates synapse structure and function.

PGRN has an important role in regulating neurite outgrowth (Gao et al., 2010; Laird et al., 2010; Ryan et al., 2009; Van Damme et al., 2008), and neuronal activity might be a key factor in modulating the manner in which PGRN exerts its effects on neuronal arborization. For instance, acute increases in BDNF concentration and resulting transient activation of TrkB enhances neurite elongation and spine head enlargement (Ji et al., 2010). Conversely, gradual increases in BDNF concentration and sustained TrkB activation promote neurite branching and spine neck elongation (Ji et al., 2010). In addition, local acute applications of BDNF to the neurites of cultured hippocampal neurons have been demonstrated to induce axon differentiation (Shelly et al., 2007). It is yet unknown how changes in the concentration of PGRN and the location of PGRN release impact neuronal outgrowth and synapse morphology.

We demonstrate that treatment of neurons with recombinant PGRN increases synapse density but decreases the integrated density of the presynaptic protein, VGlut-1 and the number of synaptic vesicles per synapse. It is possible that the effects of exogenous PRGN on presynapse size and synapse number might be direct or secondary to changes in neuronal or synaptic activity.

It is important to note that although treatment of cells with recombinant PGRN decreases the size of VGlut-1 puncta, and viral-mediated knockdown of PGRN in >90% of cells results in an increase in size of VGlut-1 puncta (Tapia et al., 2011), transient transfection of cells with PGRN-GFP (~1% of cells transfected) did not significantly change the size of VGlut-1 puncta (Tapia et al., 2011). This suggests that PGRN-mediated changes in VGlut-1 size are not cell autonomous and are probably regulated by levels of postsynaptic PGRN. This is in accordance with previous evidence demonstrating an important role for PGRN in regulating neuronal connectivity and synaptic plasticity (Petkau et al., 2012; Tapia et al., 2011). We postulate that activity-mediated secretion of PGRN regulates the number and morphology of synaptic connections. However, many important questions remain unanswered. Does PGRN exert different effects when secreted synaptically and extrasynaptically? Does PGRN act locally or globally once secreted in response to neuronal activity? Does PGRN exert differential effects when secreted presynaptically or postsynaptically, and do the time course and pattern of secretion impact its actions? Answers to these questions will provide further understanding of the basic biology of PGRN, which is greatly needed to further our understanding of the pathophysiology of FTD.

Materials and Methods

DNA constructs

PGRN-GFP

The human PGRN cDNA (accession no. NM_002087) was a kind gift from Max Cynader (University of British Columbia, BC, Canada). The PGRN–GFP fusion protein was generated by amplifying the PGRN coding sequence without the stop codon for cloning into JPA7-GFP (Sampo et al., 2003). The forward primer included a *Hin*dIII restriction site (underlined): 5′-TCTAAGCTTGCGCC-AAGATGTGGACCCTG-3′. The reverse primer incorporated an *Age*I site (underlined) in addition to changing the STOP codon to a glycine (in bold): 5′-CGACCGGTATTCC**TCC**CAGCAGCTGTCTC-3′. Plasmid composition was confirmed by sequencing.

PGRN-superecliptic pHluorin (PGRN–SEP)

Superecliptic pHluorin (SEP; accession no. AY533296; a kind gift from Michael Ehlers, Duke University, Durham, NC) was PCR amplified: forward, 5′-ACCGGTCATGAGTAAAGGAG-3′; reverse, 5′-TCTAGAATTATTTGTATAG-TTCA-3′. It was then subcloned into the pJPA7 vector replacing GFP to produce PGRN-SEP.

Other constructs

BDNF-RFP was a kind gift from Gary Banker (Oregon Health and Science University, Portland, OR) chromograninA-RFP was a kind gift from Laurent Taupenot (NIH), and PSD-95-RFP and synRFP were kind gifts from David Bredt and Louis Reichardt (University of California, San Francisco, CA).

Hippocampal culture and transfection

Primary hippocampal cultures were prepared from embryonic day 18 (E18) Sprague Dawley rats as previously described (Xie et al., 2000) or from E16 C57Bl/6 mice also as previously described (Kaech and Banker, 2006). Neurons were plated at a density of 197 cells/mm^2 and 46 cells/mm^2, respectively, and maintained in Neurobasal/B27 (Invitrogen, Carlsbad, CA). Neurons were transfected using Lipofectamine 2000 (Invitrogen, Carlsbad, CA) at 9–10 days *in vitro* (DIV) according to the manufacturer's protocol and imaged at 10–11 or 13–16 DIV.

Activity treatments

High K^+ (51.5 mM NaCl, 70 mM KCl, 2 mM $CaCl_2$, 2 mM $MgCl_2$, 25 mM HEPES and 30 mM glucose, pH 7.4); 4-aminopyridine (4-AP) and bicuculline (119 mM NaCl, 2.5 mM KCl, 0.5 mM $CaCl_2$, 3.5 mM $MgCl_2$, 25 mM HEPES, 30 mM glucose, 0.5 mM 4-AP and 10 µM bicuculline, pH 7.4); $CdCl_2$ treatment (119 mM NaCl, 2.5 mM KCl, 0.5 mM $CaCl_2$, 3.5 mM $MgCl_2$, 25 mM HEPES, 30 mM glucose and 100 µM $CdCl_2$, pH 7.4); calcium-free medium (119 mM NaCl, 2.5 mM KCl, 7 mM $MgCl_2$, 25 mM HEPES, 30 mM glucose and 100 µM EGTA, pH 7.4); high K^+ and $CdCl_2$ treatment (51.5 mM NaCl, 70 mM KCl, 2 mM $CaCl_2$, 2 mM $MgCl_2$, 25 mM HEPES, 30 mM glucose and 100 µM $CdCl_2$, pH 7.4); high K^+ in calcium-free medium (51.5 mM NaCl, 70 mM KCl, 4 mM $MgCl_2$, 25 mM HEPES, 30 mM glucose and 100 µM EGTA, pH 7.4); 4-AP and bicuculline and $CdCl_2$ treatment (119 mM NaCl, 2.5 mM KCl, 0.5 mM $CaCl_2$, 3.5 mM $MgCl_2$, 25 mM HEPES, 30 mM glucose, 0.5 mM 4-AP, 10 µM bicuculline and 100 µM $CdCl_2$, pH 7.4); 4-AP and bicuculline in calcium-free medium (119 mM NaCl, 2.5 mM KCl, 7 mM $MgCl_2$, 25 mM HEPES, 30 mM glucose, 0.5 mM 4-AP, 10 µM bicuculline and 100 µM EGTA, pH 7.4).

To validate pH-dependent SEP, cells were first treated with a solution containing NH_4Cl (pH 7.4), and then with one containing 2-(*N*-morpholino)ethanesulfonic acid (MES). 50 mM NaCl was substituted for 50 mM NH_4Cl, and all other components remained the same as in the control solution, with the pH adjusted to 7.4. For the treatment with acidic MES solution, 25 mM HEPES was replaced with 25 mM MES and all other components remained unchanged; the pH was adjusted to 5.2. The average PGRN–SEP fluorescent event density was calculated by dividing the total number of PGRN–SEP fluorescent events in each frame by the total neurite length, and averaging for all the frames in the 10 minute time-lapse imaging series. The number of PGRN–SEP fluorescent events was manually counted for each of the time-lapse images. All visible puncta more than 2 pixels in size were counted. Colocalization of PGRN–SEP fluorescent puncta and synRFP or PSD-95–RFP puncta was determined by manually counting all overlapping puncta (>1 pixel overlap) in each frame.

Recombinant PGRN treatment

Neurons were treated with recombinant PGRN protein (R&D Systems, Minneapolis, MN) at concentrations of 0, 100 and 250 ng/ml on 0, 3, 7 and 10 DIV. Synapse density and size were analyzed at 14 DIV.

Immunohistochemistry

Cultures were fixed with 4% paraformaldehyde and 4% sucrose for 10 minutes, permeabilized with 0.1% Triton-X for 10 minutes, and blocked with 10% goat serum for 1 hour at room temperature. Primary and secondary antibodies were diluted in 1% goat serum in PBS. Cells were incubated in primary antibody at 4℃ overnight, and in secondary antibody for 1 hour at room temperature. Primary antibodies: rabbit anti-PGRN (Invitrogen, Carlsbad, CA), rabbit anti-MAP2 (Abcam, San Francisco, CA), guinea pig anti-VGlut-1 (Millipore, Billerica, MA), mouse anti-PSD-95 (Affinity BioReagents, Golden, CO), mouse anti-SGII (Santa Cruz Biotech, Santa Cruz, CA). Secondary antibodies: Alexa Fluor 488, Texas Red or Cy5-conjugated goat anti-rabbit, anti-mouse or anti-guinea pig (Molecular Probes, Eugene, OR).

Electron microscopy

Hippocampal cultures were plated on Aclar membrane inserts in a multiwell chamber (Costar) treated with poly-L-lysine. At 13 DIV, cells were fixed and embedded in JEMBED and Spurr's resin. Grids were cut and stained with 2% uranyl acetate and Reynold's lead. Over 50 separate images (magnification 50,000×) were acquired for each treatment and analyzed with the experimenter blind to the experimental condition.

Image acquisition

Imaging of PGRN–GFP and BDNF–RFP transport, as well as endogenous PGRN immunostaining, were done under 63× magnification on a standard wide-field fluorescence DMI 6000 B Leica microscope equipped with a cooled CCD camera and controlled by MetaMorph software as previously described (Kwinter and Silverman, 2009). Imaging for all other experiments was done using an inverted confocal Olympus FV1000 microscope (60×/1.4 NA oil Plan-Apochromat). All images in a given experiment were captured and analyzed using the same exposure time and conditions.

Image analysis

Transport of PGRN–GFP and BDNF–RFP

14 DIV neurons transfected with PGRN–GFP and BDNF–RFP were imaged using time-lapse imaging at 37℃. Streamed recordings were made of transport events along a section of the axon using the cell body to determine anterograde and retrograde directions of transport. The output files were distance–time plots (kymographs) of transport events, which were manually traced on MetaMorph. Anterograde and retrograde events were traced separately. Each trace consisted of a run ≥2 μm in length and stopped if the vesicle remained stationary for four or more frames. Custom software was then used to calculate the parameters of vesicle flux, velocity and run length (Kwinter et al., 2009). Vesicle flux was defined as the sum of the distances traveled by all vesicles, standardized by the length and duration of each recording.

PGRN colocalization (density of colocalized clusters)

Images of PGRN–GFP and BDNF–RFP were thresholded separately by subjectively evaluating real clusters using ImageJ. The established threshold was then applied to all images across experimental groups to enable unbiased analysis. The density of puncta was calculated by dividing the total number of PGRN–GFP or BDNF–RFP puncta by the total neurite length. Points of colocalization were determined using the ImageJ colocalization plugin (http://rsb.info.nih.gov/ij/plugins/colocalization.html). Points of colocalization were defined as regions >4 pixels in size where the intensity ratio of the two channels was >50.

Percent PGRN colocalization

Images of PGRN or PGRN–GFP plus chromograninA–RFP or SGII were analyzed as above. Percentage colocalization was quantified by dividing the total number of colocalized puncta by the number of PGRN puncta.

PGRN–GFP punctum area and integrated density

Neurons expressing PGRN–GFP and synRFP were treated with 0.5 mM 4-aminopyridine (4-AP) and 10 μM bicuculline and imaged 5 and 10 minutes after treatment. Images were thresholded using ImageJ. Puncta were thresholded subjectively, and the appropriate threshold was applied to all the images in the experiment. PGRN–GFP punctum area and integrated density (IntDen; product of the area and the mean gray value) were then determined before and after treatment of cells using ImageJ.

Analysis of PGRN–GFP at synapses

To determine the integrated density of synaptic PGRN–GFP puncta, PGRN–GFP puncta that colocalized with synRFP were identified in Adobe Photoshop and analyzed. All PGRN–GFP puncta not associated with synRFP were similarly analyzed in a separate pool.

Synapse density

Masks of GFP-transfected neurons were made using Adobe Photoshop, enabling the visualization of all VGlut-1 and PSD-95 immunolabeling associated with the transfected cell. Images of VGlut-1 and PSD-95 immunolabeling were then thresholded using ImageJ. Puncta were thresholded subjectively, but once the appropriate threshold was selected, it was applied to all the images in the experiment. Points of colocalization were analyzed using the ImageJ colocalization plugin.

Live imaging of PGRN–SEP

Neurons transfected with PGRN-SEP and synRFP or BDNF-RFP were imaged every 12 seconds at 37℃. Neurons were initially imaged for 5 minutes in a control solution (119 mM NaCl, 2.5 mM KCl, 0.5 mM $CaCl_2$, 3.5 mM $MgCl_2$, 25 mM HEPES and 30 mM glucose, pH 7.4). After 5 minutes of imaging, cells were switched to the various treatments and imaged for an additional 10 minutes.

Author contributions

E.P., S.F., F.M., F.S. and D.H. did all experiments. C.K., M.A.S. and S.X.B. conceived and supervised the study.

Funding

This work was supported by grants from the Canadian Institutes of Health Research [grant numbers MOP-81158 to S.X.B. and MOP-90396 to M.A.S.], the National Science and Engineering Research Council of Canada [grant numbers 327100-06 to M.A.S., 171372-06 to C.K.]; the Canadian Foundation for Innovation [grant number 12793 to MAS]; and the Alzheimer's Society of Canada [grant number 12_123 to S.X.B.].

Supplementary material available online at
http://jcs.biologists.org/lookup/suppl/doi:10.1242/jcs.132076/-/DC1

References

Adachi, N., Kohara, K. and Tsumoto, T. (2005). Difference in trafficking of brain-derived neurotrophic factor between axons and dendrites of cortical neurons, revealed by live-cell imaging. *BMC Neurosci.* **6**, 42.

Alkadhi, K. A. and Hogan, Y. H. (1989). Effect of calcium on synaptic facilitation by potassium channel blockers in superior cervical ganglion of rat. *Neuropharmacology* **28**, 75-81.

Baker, M., Mackenzie, I. R., Pickering-Brown, S. M., Gass, J., Rademakers, R., Lindholm, C., Snowden, J., Adamson, J., Sadovnick, A. D., Rollinson, S. et al. (2006). Mutations in progranulin cause tau-negative frontotemporal dementia linked to chromosome 17. *Nature* **442**, 916-919.

Balkowiec, A. and Katz, D. M. (2002). Cellular mechanisms regulating activity-dependent release of native brain-derived neurotrophic factor from hippocampal neurons. *J. Neurosci.* **22**, 10399-10407.

Barkus, R. V., Klyachko, O., Horiuchi, D., Dickson, B. J. and Saxton, W. M. (2008). Identification of an axonal kinesin-3 motor for fast anterograde vesicle transport that facilitates retrograde transport of neuropeptides. *Mol. Biol. Cell* **19**, 274-283.

Bateman, A. and Bennett, H. P. (2009). The granulin gene family: from cancer to dementia. *Bioessays* **31**, 1245-1254.

Bronner, I. F., Rizzu, P., Seelaar, H., van Mil, S. E., Anar, B., Azmani, A., Donker Kaat, L., Rosso, S., Heutink, P. and van Swieten, J. C. (2007). Progranulin mutations in Dutch familial frontotemporal lobar degeneration. *Eur. J. Hum. Genet.* **15**, 369-374.

Cruts, M., Gijselinck, I., van der Zee, J., Engelborghs, S., Wils, H., Pirici, D., Rademakers, R., Vandenberghe, R., Dermaut, B., Martin, J. J. et al. (2006). Null mutations in progranulin cause ubiquitin-positive frontotemporal dementia linked to chromosome 17q21. *Nature* **442**, 920-924.

Curtis, D. R., Duggan, A. W., Felix, D. and Johnston, G. A. (1970). GABA, bicuculline and central inhibition. *Nature* **226**, 1222-1224.

de Jong, E. K., Vinet, J., Stanulovic, V. S., Meijer, M., Wesseling, E., Sjollema, K., Boddeke, H. W. and Biber, K. (2008). Expression, transport, and axonal sorting of neuronal CCL21 in large dense-core vesicles. *FASEB J.* **22**, 4136-4145.

Dean, C., Liu, H., Dunning, F. M., Chang, P. Y., Jackson, M. B. and Chapman, E. R. (2009). Synaptotagmin-IV modulates synaptic function and long-term potentiation by regulating BDNF release. *Nat. Neurosci.* **12**, 767-776.

Dean, C., Liu, H., Staudt, T., Stahlberg, M. A., Vingill, S., Bückers, J., Kamin, D., Engelhardt, J., Jackson, M. B., Hell, S. W. et al. (2012). Distinct subsets of Syt-IV/BDNF vesicles are sorted to axons versus dendrites and recruited to synapses by activity. *J. Neurosci.* **32**, 5398-5413.

Dieni, S., Matsumoto, T., Dekkers, M., Rauskolb, S., Ionescu, M. S., Deogracias, R., Gundelfinger, E. D., Kojima, M., Nestel, S., Frotscher, M. et al. (2012). BDNF and

its pro-peptide are stored in presynaptic dense core vesicles in brain neurons. *J. Cell Biol.* **196**, 775-788.

Gandhi, S. P. and Stevens, C. F. (2003). Three modes of synaptic vesicular recycling revealed by single-vesicle imaging. *Nature* **423**, 607-613.

Gao, X., Joselin, A. P., Wang, L., Kar, A., Ray, P., Bateman, A., Goate, A. M. and Wu, J. Y. (2010). Progranulin promotes neurite outgrowth and neuronal differentiation by regulating GSK-3β. *Protein Cell* **1**, 552-562.

Gass, J., Cannon, A., Mackenzie, I. R., Boeve, B., Baker, M., Adamson, J., Crook, R., Melquist, S., Kuntz, K., Petersen, R. et al. (2006). Mutations in progranulin are a major cause of ubiquitin-positive frontotemporal lobar degeneration. *Hum. Mol. Genet.* **15**, 2988-3001.

Gauthier, L. R., Charrin, B. C., Borrell-Pagès, M., Dompierre, J. P., Rangone, H., Cordelières, F. P., De Mey, J., MacDonald, M. E., Lessmann, V., Humbert, S. et al. (2004). Huntingtin controls neurotrophic support and survival of neurons by enhancing BDNF vesicular transport along microtubules. *Cell* **118**, 127-138.

Goodman, L. J., Valverde, J., Lim, F., Geschwind, M. D., Federoff, H. J., Geller, A. I. and Hefti, F. (1996). Regulated release and polarized localization of brain-derived neurotrophic factor in hippocampal neurons. *Mol. Cell. Neurosci.* **7**, 222-238.

Guo, A., Tapia, L., Bamji, S. X., Cynader, M. S. and Jia, W. (2010). Progranulin deficiency leads to enhanced cell vulnerability and TDP-43 translocation in primary neuronal cultures. *Brain Res.* **1366**, 1-8.

Hardingham, G. E., Fukunaga, Y. and Bading, H. (2002). Extrasynaptic NMDARs oppose synaptic NMDARs by triggering CREB shut-off and cell death pathways. *Nat. Neurosci.* **5**, 405-414.

Hartmann, M., Heumann, R. and Lessmann, V. (2001). Synaptic secretion of BDNF after high-frequency stimulation of glutamatergic synapses. *EMBO J.* **20**, 5887-5897.

Hoey, S. E., Williams, R. J. and Perkinton, M. S. (2009). Synaptic NMDA receptor activation stimulates alpha-secretase amyloid precursor protein processing and inhibits amyloid-beta production. *J. Neurosci.* **29**, 4442-4460.

Jakawich, S. K., Nasser, H. B., Strong, M. J., McCartney, A. J., Perez, A. S., Rakesh, N., Carruthers, C. J. and Sutton, M. A. (2010). Local presynaptic activity gates homeostatic changes in presynaptic function driven by dendritic BDNF synthesis. *Neuron* **68**, 1143-1158.

Ji, Y., Lu, Y., Yang, F., Shen, W., Tang, T. T., Feng, L., Duan, S. and Lu, B. (2010). Acute and gradual increases in BDNF concentration elicit distinct signaling and functions in neurons. *Nat. Neurosci.* **13**, 302-309.

Kaech, S. and Banker, G. (2006). Culturing hippocampal neurons. *Nat. Protoc.* **1**, 2406-2415.

Kokaia, Z., Andsberg, G., Yan, Q. and Lindvall, O. (1998). Rapid alterations of BDNF protein levels in the rat brain after focal ischemia: evidence for increased synthesis and anterograde axonal transport. *Exp. Neurol.* **154**, 289-301.

Kuriu, T., Inoue, A., Bito, H., Sobue, K. and Okabe, S. (2006). Differential control of postsynaptic density scaffolds via actin-dependent and -independent mechanisms. *J. Neurosci.* **26**, 7693-7706.

Kwinter, D. M. and Silverman, M. A. (2009). Live imaging of dense-core vesicles in primary cultured hippocampal neurons. *J. Vis. Exp.* **27**, e1144.

Kwinter, D. M., Lo, K., Mafi, P. and Silverman, M. A. (2009). Dynactin regulates bidirectional transport of dense-core vesicles in the axon and dendrites of cultured hippocampal neurons. *Neuroscience* **162**, 1001-1010.

Laird, A. S., Van Hoecke, A., De Muynck, L., Timmers, M., Van den Bosch, L., Van Damme, P. and Robberecht, W. (2010). Progranulin is neurotrophic in vivo and protects against a mutant TDP-43 induced axonopathy. *PLoS ONE* **5**, e13368.

Lessmann, V. and Brigadski, T. (2009). Mechanisms, locations, and kinetics of synaptic BDNF secretion: an update. *Neurosci. Res.* **65**, 11-22.

Lu, B., Pang, P. T. and Woo, N. H. (2005). The yin and yang of neurotrophin action. *Nat. Rev. Neurosci.* **6**, 603-614.

Mackenzie, I. R., Baker, M., Pickering-Brown, S., Hsiung, G. Y., Lindholm, C., Dwosh, E., Gass, J., Cannon, A., Rademakers, R., Hutton, M. et al. (2006). The neuropathology of frontotemporal lobar degeneration caused by mutations in the progranulin gene. *Brain* **129**, 3081-3090.

Matsuda, N., Lu, H., Fukata, Y., Noritake, J., Gao, H., Mukherjee, S., Nemoto, T., Fukata, M. and Poo, M. M. (2009). Differential activity-dependent secretion of brain-derived neurotrophic factor from axon and dendrite. *J. Neurosci.* **29**, 14185-14198.

Matzilevich, D. A., Rall, J. M., Moore, A. N., Grill, R. J. and Dash, P. K. (2002). High-density microarray analysis of hippocampal gene expression following experimental brain injury. *J. Neurosci. Res.* **67**, 646-663.

Mellman, I., Fuchs, R. and Helenius, A. (1986). Acidification of the endocytic and exocytic pathways. *Annu. Rev. Biochem.* **55**, 663-700.

Miesenböck, G., De Angelis, D. A. and Rothman, J. E. (1998). Visualizing secretion and synaptic transmission with pH-sensitive green fluorescent proteins. *Nature* **394**, 192-195.

Mukherjee, O., Pastor, P., Cairns, N. J., Chakraverty, S., Kauwe, J. S., Shears, S., Behrens, M. I., Budde, J., Hinrichs, A. L., Norton, J. et al. (2006). HDDD2 is a familial frontotemporal lobar degeneration with ubiquitin-positive, tau-negative inclusions caused by a missense mutation in the signal peptide of progranulin. *Ann. Neurol.* **60**, 314-322.

Mukherjee, O., Wang, J., Gitcho, M., Chakraverty, S., Taylor-Reinwald, L., Shears, S., Kauwe, J. S., Norton, J., Levitch, D., Bigio, E. H. et al. (2008). Molecular characterization of novel progranulin (GRN) mutations in frontotemporal dementia. *Hum. Mutat.* **29**, 512-521.

Njus, D., Kelley, P. M. and Harnadek, G. J. (1986). Bioenergetics of secretory vesicles. *Biochim. Biophys. Acta* **853**, 237-265.

Pease, M. E., McKinnon, S. J., Quigley, H. A., Kerrigan-Baumrind, L. A. and Zack, D. J. (2000). Obstructed axonal transport of BDNF and its receptor TrkB in experimental glaucoma. *Invest. Ophthalmol. Vis. Sci.* **41**, 764-774.

Petkau, T. L., Neal, S. J., Orban, P. C., MacDonald, J. L., Hill, A. M., Lu, G., Feldman, H. H., Mackenzie, I. R. and Leavitt, B. R. (2010). Progranulin expression in the developing and adult murine brain. *J. Comp. Neurol.* **518**, 3931-3947.

Petkau, T. L., Neal, S. J., Milnerwood, A., Mew, A., Hill, A. M., Orban, P., Gregg, J., Lu, G., Feldman, H. H., Mackenzie, I. R. et al. (2012). Synaptic dysfunction in progranulin-deficient mice. *Neurobiol. Dis.* **45**, 711-722.

Pickering-Brown, S. M., Baker, M., Gass, J., Boeve, B. F., Loy, C. T., Brooks, W. S., Mackenzie, I. R., Martins, R. N., Kwok, J. B., Halliday, G. M. et al. (2006). Mutations in progranulin explain atypical phenotypes with variants in MAPT. *Brain* **129**, 3124-3126.

Poon, W. W., Blurton-Jones, M., Tu, C. H., Feinberg, L. M., Chabrier, M. A., Harris, J. W., Jeon, N. L. and Cotman, C. W. (2011). β-Amyloid impairs axonal BDNF retrograde trafficking. *Neurobiol. Aging* **32**, 821-833.

Roux, J. C., Zala, D., Panayotis, N., Borges-Correia, A., Saudou, F. and Villard, L. (2012). Modification of Mecp2 dosage alters axonal transport through the Huntingtin/Hap1 pathway. *Neurobiol. Dis.* **45**, 786-795.

Ryan, C. L., Baranowski, D. C., Chitramuthu, B. P., Malik, S., Li, Z., Cao, M., Minotti, S., Durham, H. D., Kay, D. G., Shaw, C. A. et al. (2009). Progranulin is expressed within motor neurons and promotes neuronal cell survival. *BMC Neurosci.* **10**, 130.

Sampo, B., Kaech, S., Kunz, S. and Banker, G. (2003). Two distinct mechanisms target membrane proteins to the axonal surface. *Neuron* **37**, 611-624.

Sankaranarayanan, S., De Angelis, D., Rothman, J. E. and Ryan, T. A. (2000). The use of pHluorins for optical measurements of presynaptic activity. *Biophys. J.* **79**, 2199-2208.

Santi, S., Cappello, S., Riccio, M., Bergami, M., Aicardi, G., Schenk, U., Matteoli, M. and Canossa, M. (2006). Hippocampal neurons recycle BDNF for activity-dependent secretion and LTP maintenance. *EMBO J.* **25**, 4372-4380.

Shakiryanova, D., Tully, A. and Levitan, E. S. (2006). Activity-dependent synaptic capture of transiting peptidergic vesicles. *Nat. Neurosci.* **9**, 896-900.

Shankaran, S. S., Capell, A., Hruscha, A. T., Fellerer, K., Neumann, M., Schmid, B. and Haass, C. (2008). Missense mutations in the progranulin gene linked to frontotemporal lobar degeneration with ubiquitin-immunoreactive inclusions reduce progranulin production and secretion. *J. Biol. Chem.* **283**, 1744-1753.

Shelly, M., Cancedda, L., Heilshorn, S., Sumbre, G. and Poo, M. M. (2007). LKB1/STRAD promotes axon initiation during neuronal polarization. *Cell* **129**, 565-577.

Tang, W., Lu, Y., Tian, Q. Y., Zhang, Y., Guo, F. J., Liu, G. Y., Syed, N. M., Lai, Y., Lin, E. A., Kong, L. et al. (2011). The growth factor progranulin binds to TNF receptors and is therapeutic against inflammatory arthritis in mice. *Science* **332**, 478-484.

Tapia, L., Milnerwood, A., Guo, A., Mills, F., Yoshida, E., Vasuta, C., Mackenzie, I. R., Raymond, L., Cynader, M., Jia, W. et al. (2011). Progranulin deficiency decreases gross neural connectivity but enhances transmission at individual synapses. *J. Neurosci.* **31**, 11126-11132.

Tongiorgi, E., Righi, M. and Cattaneo, A. (1997). Activity-dependent dendritic targeting of BDNF and TrkB mRNAs in hippocampal neurons. *J. Neurosci.* **17**, 9492-9505.

Van Damme, P., Van Hoecke, A., Lambrechts, D., Vanacker, P., Bogaert, E., van Swieten, J., Carmeliet, P., Van Den Bosch, L. and Robberecht, W. (2008). Progranulin functions as a neurotrophic factor to regulate neurite outgrowth and enhance neuronal survival. *J. Cell Biol.* **181**, 37-41.

van der Zee, J., Le Ber, I., Maurer-Stroh, S., Engelborghs, S., Gijselinck, I., Camuzat, A., Brouwers, N., Vandenberghe, R., Sleegers, K., Hannequin, D. et al. (2007). Mutations other than null mutations producing a pathogenic loss of progranulin in frontotemporal dementia. *Hum. Mutat.* **28**, 416.

Wang, J., Van Damme, P., Cruchaga, C., Gitcho, M. A., Vidal, J. M., Seijo-Martínez, M., Wang, L., Wu, J. Y., Robberecht, W. and Goate, A. (2010). Pathogenic cysteine mutations affect progranulin function and production of mature granulins. *J. Neurochem.* **112**, 1305-1315.

Xie, C., Markesbery, W. R. and Lovell, M. A. (2000). Survival of hippocampal and cortical neurons in a mixture of MEM+ and B27-supplemented neurobasal medium. *Free Radic. Biol. Med.* **28**, 665-672.

Xu, J., Xilouri, M., Bruban, J., Shioi, J., Shao, Z., Papazoglou, I., Vekrellis, K. and Robakis, N. K. (2011). Extracellular progranulin protects cortical neurons from toxic insults by activating survival signaling. *Neurobiol Aging* **32**, 2326.e5-2326.e16.